

Dihydroazulene Photoswitch Operating in Sequential Tunneling Regime: Synthesis and Single-Molecule Junction Studies

Søren Lindbæk Broman, Samuel Lara-Avila, Christine Lindbjerg Thisted, Andrew D. Bond, Sergey Kubatkin, Andrey Danilov,* and Mogens Brøndsted Nielsen*

Molecular switches play a central role for the development of molecular electronics. In this work it is demonstrated that the reproducibility and robustness of a single-molecule dihydroazulene (DHA)/vinylheptafulvene (VHF) switch can be remarkably enhanced if the switching kernel is weakly coupled to electrodes so that the electron transport goes by sequential tunneling. To assure weak coupling, the DHA switching kernel is modified by incorporating *p*-MeSC₆H₄ end-groups. Molecules are prepared by Suzuki cross-couplings on suitable halogenated derivatives of DHA. The synthesis presents an expansion of our previously reported bromination–elimination–cross-coupling protocol for functionalization of the DHA core. For all new derivatives the kinetics of DHA/VHF transition has been thoroughly studied in solution. The kinetics reveals the effect of sulfur end-groups on the thermal ring-closure of VHF. One derivative, incorporating a *p*-MeSC₆H₄ anchoring group in one end, has been placed in a silver nanogap. Conductance measurements justify that transport through both DHA (high resistivity) and VHF (low resistivity) forms goes by sequential tunneling. The switching is fairly reversible and reenterable; after more than 20 “ON-OFF” switchings, both DHA and VHF forms are still recognizable, albeit noticeably different from the original states.

1. Introduction

Molecular electronics aims at using tailor-built molecules as active device elements to achieve a desired electronic functionality.^[1] Conventional computing operations can be performed by a single molecule working as a transistor or as a logical switch.

S. L. Broman, C. L. Thisted, Prof. M. B. Nielsen
Department of Chemistry
University of Copenhagen
Universitetsparken 5, DK-2100 Copenhagen Ø, Denmark
E-mail: mbn@kiku.dk

S. Lara-Avila, Prof. S. Kubatkin, Dr. A. Danilov
Department of Microtechnology and Nanoscience
Chalmers University of Technology
Kemivägen 9, S-41296 Göteborg, Sweden
E-mail: andrey.danilov@chalmers.se

Prof. A. D. Bond
Department of Physics, Chemistry and Pharmacy
University of Southern Denmark
Campusvej 55, DK-5230 Odense M, Denmark

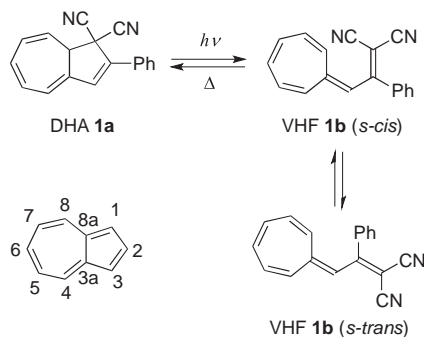


DOI: 10.1002/adfm.201200897

Light provides an attractive external stimulus for triggering molecular conductivity changes, and one of the long standing challenges in the field is to build reliable single-molecule photoswitch. While for voltage-controlled molecular switches durable operation involving more than 10⁵ ON-OFF cycles has already been demonstrated,^[2] none of the single-molecule photoswitches can compete with Complementary Metal–Oxide–Semiconductor (CMOS) devices. There are several examples^[3] of reversible switching of photosensitive dithienylethene and azobenzene molecules placed in a solid state device, like a nanogap between planar electrodes, but in some cases quenching of the excited state is observed or the molecule stopped responding to light after a few transitions if they could rearrange on the surface. Theoretical studies have indicated that a strong coupling is likely responsible for the quenching of molecular states.^[4] This idea was supported experimentally by reducing the coupling between the

electrode and the molecule, simply by moving the anchoring group (thiol) to the *meta* position of the aryl unit linked to the photoswitch.^[3b,g] Along the same line, in our recent study on the dihydroazulene (DHA)/vinylheptafulvene (VHF) photo-/thermoswitch,^[5] we argued that the operation of a photoswitch in the coherent transport regime, implying strong coupling of molecular orbitals to electrodes, should result in a short residence time for the photo-excited electron. Thus, only a small fraction of excited electrons reside on the molecule long enough time to trigger the conversion. Moreover, a tiny variation in contact geometry can affect coupling and therefore photosensitivity.

With the objective to expand the number of useful photoswitches for molecular electronics, each with their unique properties and advantages, we have focused attention on the DHA/VHF system. **Scheme 1** shows the switching events of the 2-phenyl-substituted derivatives. DHA **1a** undergoes a light-induced ring-opening reaction to generate VHF **1b**, which, in turn, undergoes a thermally-induced ring-closure to form DHA.^[6] We shall in general use letters **a** and **b** to denote a pair of DHA/VHF isomers. Pioneering work by Daub and



Scheme 1. Dihydroazulene (DHA)/ vinylheptafulvene (VHF) photo-/thermoswitch.

co-workers together with our recent work have previously established a good understanding of how the ring-opening and ring-closure reactions are influenced by electron withdrawing and donating groups at specific positions,^[7,8] acid/ base,^[7] redox-active groups,^[9] and Lewis acids.^[10] All these various ways of tuning the switching events make the DHA/VHF system particularly attractive for molecular electronics. Our first conductivity studies^[5] on the DHA derivative **2a**^[7a] (Figure 1) in a junction were promising, but also showed room for improvement. The ring-opening time for a related DHA was found to be 1.2 ps,^[11] which is much longer than the electron residence time of about ~40 fs measured for **2a** in the single-molecule junction.^[5] As a result, we found that some DHA junctions of **2a** were not photo-sensitive at all, and even those which originally responded to light, lost any photosensitivity after a few ON-OFF cycles. This is likely to occur due to a rearrangement of the molecule-to-electrode interface which, after a few switching events, reduces to the most favourable and therefore most strongly-coupled geometry.

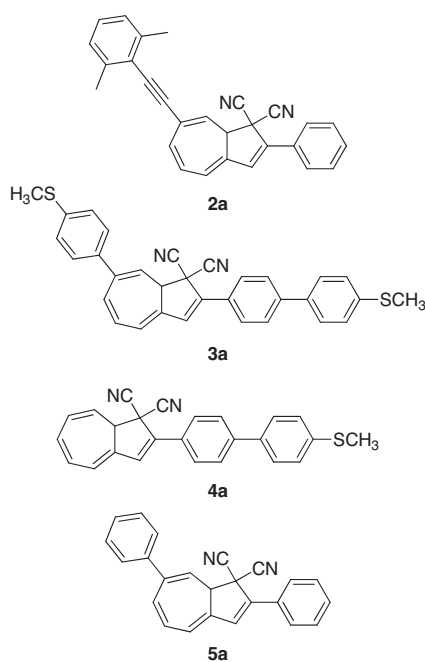


Figure 1. DHA derivatives.

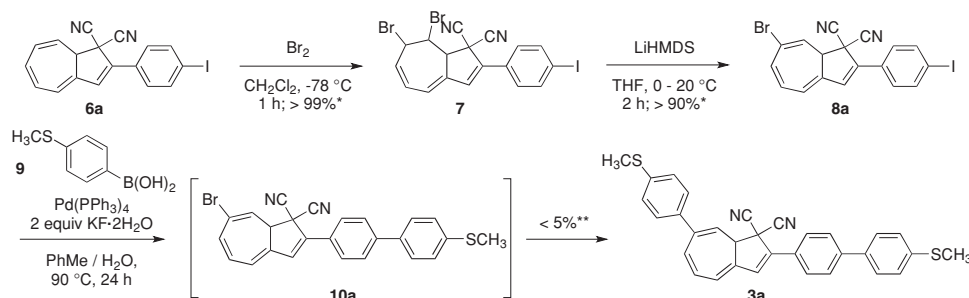
The failure to build reproducible and robust photoswitch devices operating in a strongly-coupled regime motivated us to turn to molecular junctions operating in Coulomb blockade regime. In this regime, transport through the molecule goes via sequential tunneling:^[12] an electron first jumps onto the molecule, resides there for a time which is long in the scale of molecular relaxation processes and leaves to the other electrode by the second jump. In this paper we describe the synthesis, via Suzuki cross-couplings, of new DHA derivatives **3a** and **4a** (Figure 1) suitable as molecular kernels for photoswitches operating in weakly coupled regime, achieved by using methylsulfides as anchoring groups. Thiols are often chosen as anchoring groups for adhering the molecule between two gold or silver electrodes.^[13] Usually, the thiol is protected with a readily cleavable acetyl group, which results in a strong coupling to electrodes. A weaker coupling between the electrodes and the molecule can be achieved by alkylsulfides,^[14,15] which were therefore chosen as anchoring groups in target molecules **3a** and **4a**. Additionally, we present measurements on a single-molecule switch fabricated with one particular derivative, compound **4a**, where transport, as expected, is in the Coulomb blockade regime for both ON and OFF states. We demonstrate that photosensitivity is at least an order of magnitude higher than for the non-capped DHA **2a** and does not degrade after many ON-OFF transitions. Moreover, we have performed detailed switching studies in solution revealing the electronic effect of the MeS group on the thermal ring-closure reaction.

The experimental technique for fabricating the single-molecule junction relies upon the evaporation of the molecule in ultra-high vacuum onto a substrate with a prefabricated nanogap between silver electrodes. In addition to the recent studies on DHA **2a**,^[5] the technique has previously been employed successfully for studying oligo(phenylenevinylene)s^[15] and fullerene-based^[16] and anthraquinone switches.^[17] The advantage of the technique is that no solution chemistry is involved during fabrication; the electrodes are deposited and the molecule is subsequently sublimed and trapped in the nanogap in the same vacuum cycle. The need, however, to sublime the molecule without decomposition imposes some constraints on its size and structure. Early attempts of subliming a DHA with an SAc anchoring group were thus not successful due to decomposition.

2. Results and Discussion

2.1. Synthesis

We have previously shown that regioselective functionalization of the seven-membered ring of DHA is possible via a bromination–elimination–cross-coupling protocol.^[7] This protocol has been used to synthesize molecules like **5a**^[7b] (Figure 1) and can be expanded to functionalization of both rings of the system, starting from a DHA including an iodophenyl group at the five-membered ring. This is demonstrated by the synthesis of **3a** as shown in Scheme 2. First, bromination of the known DHA **6a**^[18] using Br₂ in CH₂Cl₂ at –78 °C, as previously reported for the related 2-phenyl-DHA **1a**,^[7] gave the dibromide **7**. This

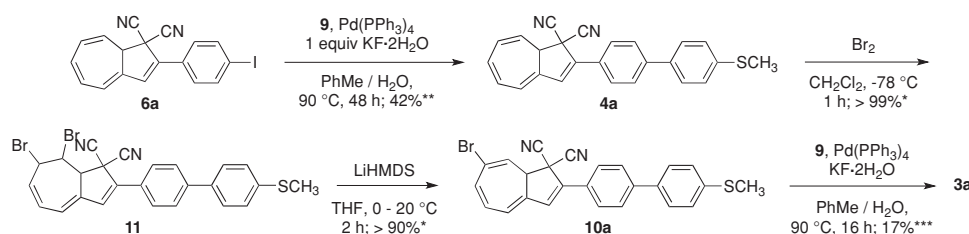


Scheme 2. Synthesis of **3a** via a double Suzuki coupling procedure. *Yields based on ^1H NMR spectroscopic analysis. **Yield calculated from **6a**.

compound was very unstable, though it was possible, however, to perform an elimination with 1 molar equivalent of lithium bis(trimethylsilyl)amide (LiHMDS) in THF to furnish the DHA **8a** in >90% purity. This compound could not easily be purified without significant loss of material, and it was therefore used crude for further reactions. A sample was, however, purified for characterization purposes. By a Suzuki coupling in a two-phase water/toluene mixture, it was coupled with 4-(methylmercapto)phenylboronic acid **9** using KF to activate the boronic acid (while base was discarded to diminish azulene formation by elimination of $\text{HCN}^{[7,19]}$). It was found that the aryl iodide was more reactive than the vinyl bromide. Thus, by both TLC and NMR spectroscopy, the presence of the intermediate **10a** was confirmed, and it was also isolated by stopping the reaction half-way to completion. A chemoselective functionalization could be accomplished by performing the reaction at $65-75^\circ\text{C}$ with one molar equivalent of the boronic acid, albeit the reaction did not go to completion. When using two molar equivalents of boronic acid at 90°C , conversion was also observed at the bromo-position, but the outcome was unfortunately accompanied by many byproducts and significant degradation. After 24 h, a simple TLC inspection showed 4 or 5 different photochromic compounds. These consisted of the aforementioned intermediate **10a**, the doubly coupled product **3a**, the iodo-phenyl-DHA **6a**, and possibly two other compounds, of which one has been isolated and identified as **4a**. No clear evidence of better results was observed by simply adding the boronic acid or the catalyst gradually in portions. The final low yield of **3a** (at best <5%) suffered from the need of purifying it by repeated chromatography (performed in the dark to avoid light-induced ring-opening), and it does not reflect the efficiency of the reaction.

To improve the yield and ease the purification, we turned to another strategy, in which the *p*- MeSC_6H_4 group was first attached to the five-membered ring of the DHA. Thus, subjecting **6a** and the boronic acid **9** to Suzuki conditions gave **4a** in high yield (**Scheme 3**). The coupling can be accomplished at room temperature with a long reaction time (7 days), but a better result was observed by performing the reaction at 90°C for 48 h. The two-step bromination-elimination procedure was then performed. The dibromide **11** and bromide **10a** were prepared without bromination of the thioether. The bromide **10a** was used crude for further reactions, but a sample was purified for characterization. Its structure was also confirmed by X-ray crystallographic analysis as shown in **Figure 2**. The compound was then subjected to a Suzuki coupling with the boronic acid **9** by heating at 90°C overnight, which gave **3a** in an acceptable yield. After a tedious purification by dry column vacuum chromatography followed by a final recrystallization from either toluene/heptanes or neat acetonitrile, **3a** was obtained pure. Crystals were subjected to X-ray crystallography (**Figure 2**).

In addition, oxidation of **4a** was possible in two steps using either one or two molar equivalents of *meta*-chloroperoxybenzoic acid (*m*-CPBA) in CH_2Cl_2 , giving the sulfoxide **12a** and sulfone **13a** (**Figure 3**), respectively, in excellent yields (see SI). The structure of the sulfone **13a** was confirmed by X-ray crystallography as shown in **Figure 2**. Finally, a derivative without the methylthio substituent was prepared in order to elucidate the influence of this group in the thermally induced ring-closure of the corresponding VHF (*vide infra*). Thus, the iodo-DHA **6a** was coupled to phenyl boronic acid, which furnished the biphenyl-DHA **14a** (**Figure 3**; see SI for synthesis).



Scheme 3. Synthesis of **3a** via a two-step coupling procedure. *Yields based on ^1H NMR spectroscopic analysis. **Yield of pure compound. ***Yield of pure compound calculated from **4a**. The compound can be isolated with minor impurities in a yield of 80%. ****Yield of pure compound calculated from **4a**. The compound can be isolated with minor impurities in a yield of 85%.

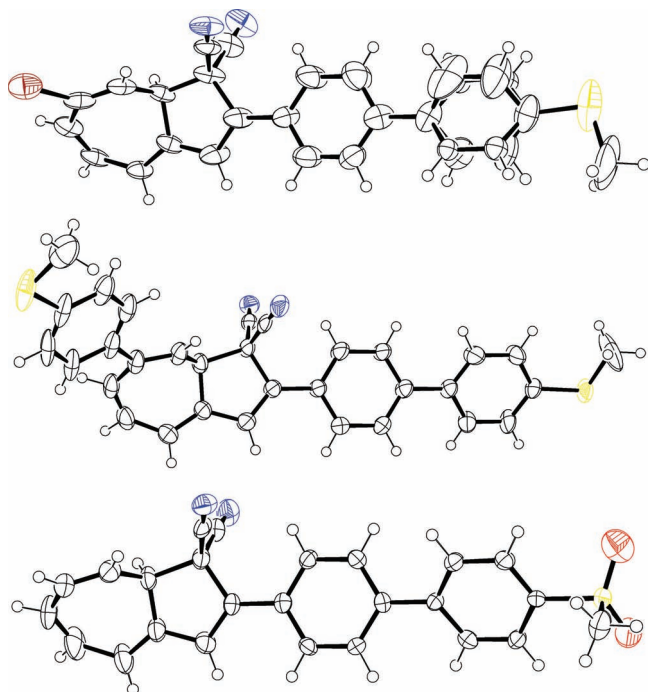


Figure 2. Molecular structures (with displacement ellipsoids at 50% probability for non-H atoms) of **10a** (top, crystals were grown from a mixture of CHCl_3 , THF, and heptanes), **3a** (middle, crystals were grown from a mixture of CHCl_3 and heptanes), and **13a** (bottom, crystals were grown from a mixture of CH_2Cl_2 / heptanes).

2.2. Solution Studies

Solution Studies. Switching studies on the DHAs **3a**, **4a**, **6a**, **8a**, **10a**, **12a**, **13a**, and **14a** were followed by UV-vis absorption spectroscopy in acetonitrile. All compounds were photochromic and underwent a light-triggered ring-opening to the corresponding VHF (as *E/Z*-isomers for those compounds with a substituent group in the heptafulvene ring; **8a**, **10a**, **3a**), which exhibited redshifted absorption maxima. Conversion of the VHF (b) to DHAs (a) occurred with isosbestic points in the absorption spectra, but with generation of isomeric mixtures of 6- and 7-substituted DHA derivatives for **8a**, **10a**, and **3a** after one light-heat cycle in the polar solvent as observed previously^[7] for related compounds (**Scheme 4**); this isomerization was confirmed by NMR spectroscopy. All compounds were stable enough to survive at least 5 full cycles of light and heat, without any sign of decomposition. Absorption maxima for the DHAs and VHF are listed in **Table 1**, and in **Figure 4** the spectra of DHAs **3a** and **4a** and their corresponding VHF **3b** and **4b** are shown. For DHA **4a** and VHF **4b**, the differences in absorption

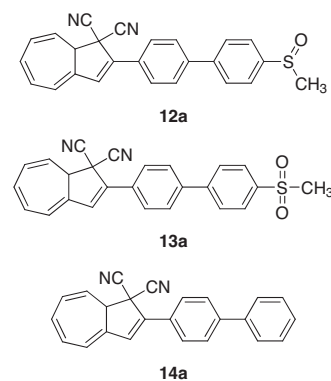
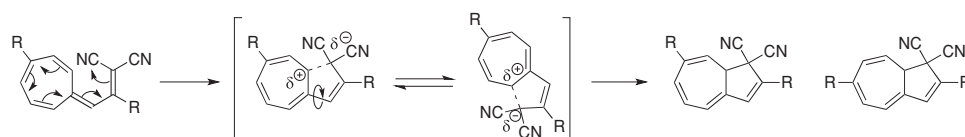


Figure 3. DHA reference compounds.

maxima correspond to a difference in the HOMO-LUMO gap of 0.69 eV.

Kinetics data for the thermally induced VHF to DHA ring-closures are collected in **Table 1** based on Arrhenius plots. For comparison, the data for the VHF of the parent phenyl-DHA/VHF **1a**/ **1b**^[20] and for the DHA/VHF **5a**/ **5b**^[7b] are also listed. The ring-closure reaction was investigated at different temperatures and the rate constants were obtained by fitting the decrease in the VHF absorption (and increase of DHA absorption) over time to first-order kinetics. All measured rate constants including its standard deviations are listed in SI. It was previously shown by change of solvent polarity^[6,20] and by Hammett linear free energy correlations^[7] that the thermal ring-closure of VHF occurs via a zwitterionic structure (**Scheme 4**). In accordance hereto, a VHF containing a mesomerically electron-donating *para*-methoxyphenyl substituent at the heptafulvene ring underwent faster ring-closure than VHF **1b**, while a VHF in which the methoxy substituent is moved to the opposite end of the molecule underwent ring-closure ($t_{1/2}$ 230 min) slower than VHF **1b**.^[7b] A phenyl group alone only has a small influence as revealed by comparison of VHF **1b** ($t_{1/2}$ 216 min) and VHF **5b** ($t_{1/2}$ 206 min). Nevertheless, we find a remarkable increase in the half-life of 49 min when proceeding from compound **4b** ($t_{1/2}$ 170 min) to **3b** ($t_{1/2}$ 219 min). These two compounds only differ by the presence of a *p*-MeSC₆H₄ substituent in the heptafulvene ring in **3b**. Altogether these results show that the *p*-MeSC₆H₄ substituent exerts a retarding influence when placed at this position; thus, the influence of the MeS substituent is in that respect opposite to the enhancing effect exerted by a MeO substituent at the same position. This is interesting in view of the fact that the Hammett σ_p -value for a MeS *para*-substituent is 0.00 (value recommended by McDaniel and Brown^[21]). On the other hand, only a minor effect is observed when attaching the SME on the biphenyl group at the opposite



Scheme 4. Proposed mechanism of a heat induced ring-closure of the substituted DHAs resulting in isomerization of DHAs (in MeCN).

Table 1. Measured absorption maxima for the DHAs and VHF and kinetics data for the thermal back-reaction (VHF \rightarrow DHA). Molar absorptivities of DHAs and VFHs are included in the experimental section. Wavelengths in brackets correspond to the absorption maxima of the mixture of 6- and 7-substituted DHAs obtained after one light-heat cycle. The half-life and rate constant are calculated from the Arrhenius plot.

DHA (a) / VHF (b)	λ_{DHA} [nm]	λ_{VHF} [nm]	$k_{25^\circ\text{C}}$ [s ⁻¹]	$t_{25^\circ\text{C}}$ [min]	E_a [kJ mol ⁻¹]	A [s ⁻¹]
1a/ 1b ^{a)}	353	470	5.36×10^{-5}	216	91.8 ± 0.2	6.35×10^{11}
6a/6b	361	476	7.62×10^{-5}	152	91.8 ± 0.5	9.31×10^{11}
8a/8b	362 (362)	468	1.63×10^{-5}	708	94.1 ± 0.4	5.07×10^{11}
4a/4b	376	475	6.81×10^{-5}	170	92.5 ± 0.3	11.0×10^{11}
10a/10b	380 (380)	462	1.29×10^{-5}	897	95.0 ± 0.4	5.74×10^{11}
3a/3b	376 (382)	504	5.26×10^{-5}	219	94.1 ± 0.4	16.0×10^{11}
14a/14b	368	476	6.35×10^{-5}	182	92.2 ± 0.2	8.87×10^{11}
5a/5b ^{b)}	355 (364)	490	5.6×10^{-5}	206	89.9 ± 0.2	3.2×10^{11}
13a/13b	369	477	7.43×10^{-5}	155	91.6 ± 0.4	8.38×10^{11}
12a/12b	370	477	9.71×10^{-5}	119	89.8 ± 0.9	5.30×10^{11}

^{a)}Data from Ref. [20] From the exponential decay of **1b** at 25 °C, $k_{25^\circ\text{C}} = 5.31 \times 10^{-5} \text{ s}^{-1}$ ($t_{1/2} = 218 \text{ min}$) is obtained; ^{b)}Data from Ref. [7b].

end of the molecule as revealed by comparing compounds **14a** and **4a**, which is not unreasonable owing to the non-planarity of the biphenyl. The kinetics data listed in Table 1 also signal the influence of an inductively electron-withdrawing bromo-substituent in the seven-membered ring. Thus, the presence of Br in VHF **10b** results in a significantly retarded ring-closure ($t_{1/2}$ 897 min) relative to VHF **4b** ($t_{1/2}$ 170 min). Comparison of the iodophenyl derivatives **8b** and **6b** reveals a similar rate-retarding effect of the bromo-substituent, $t_{1/2}$ 708 min vs. 152 min. This influence is in agreement with the involvement of a zwitterionic structure in the ring-closure reaction as mentioned above.

2.3. Conductance Measurements

A single-molecule junction based on DHA **4a** with one MeS anchoring group was prepared by evaporating the molecule under ultra-high vacuum onto a substrate with a prefabricated nanogap between silver electrodes, following the fabrication procedure described previously (including detailed nanogap characterization without the presence of molecules).^[15–17,22]

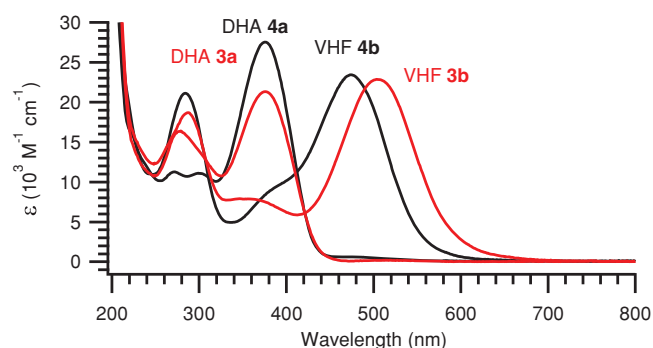


Figure 4. UV-Vis absorption spectra of DHA **3a** and its corresponding VHF **3b** (red) and DHA **4a** and its corresponding VFHs **4b** (black) measured in MeCN.

The prefabricated nanogap consisted of the source and drain electrodes of silver deposited onto a planar gate electrode made of aluminum metal covered with aluminum oxide that was prepared on a chip of oxidized silicon. DHA **3a** with two MeS anchoring groups could not be sublimed without decomposition (decomposition point 150 °C) so the studies were focused instead on **4a**. Conductance measurements were performed at 4–25 K as a function of the gate voltage, irradiation, bias potential between source and drain, and temperature. A schematic representation of the sample geometry is shown in Figure 5. It is obviously impossible to say how the molecule exactly binds, but more importantly, it is found to be weakly coupled to one electrode (*vide infra*).

The transport measurements reveal that DHA **4a** in a silver nanogap can exist in two distinct forms—A and B. First of all, the transport through the original form A was characterized by measuring the stability plot (a set of differential conductance curves taken at different gate voltages), presented in Figure 6. The stability diagram reveals a set of characteristic Coulomb blockade diamonds, which implies that the molecule is weakly coupled to electrodes and the transport through the molecule goes by sequential tunneling.^[12a] For low bias voltages (below 100 mV), the stability plot is stable and reproducible. The

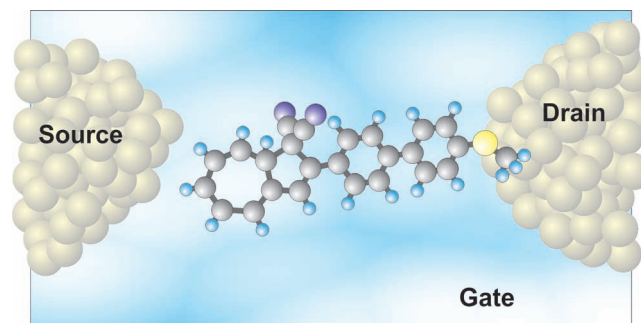


Figure 5. A schematic representation of the sample geometry of molecule **4a** anchored via the SMe group to one electrode in the silver nanogap.

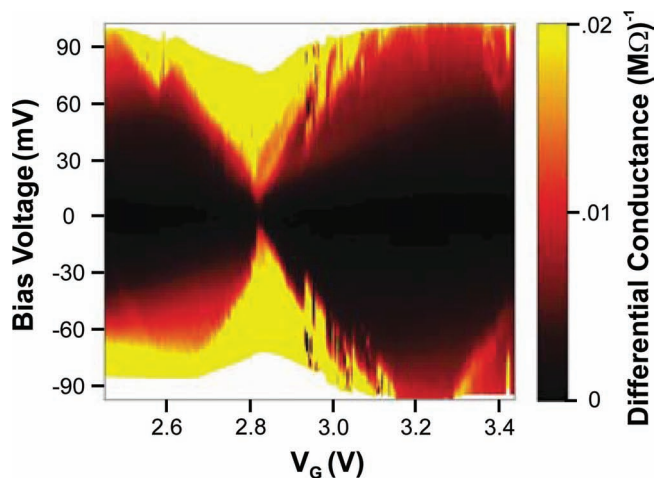


Figure 6. Stability diagram for single-molecule junction taken right after the molecule was caught in nanogap.

stability diagram taken for bias voltages up to 150 mV reveals switching from original form A to more conducting (low resistive) form B, which happens at a gate voltage around 3 V (Figure 7).

Such a behavior indicates that below $V_G^0 \approx 3$ V, the form A is the ground state, while above V_G^0 it becomes metastable. To promote switching to a new ground state (form B), high bias voltage is needed. From our measurements we cannot deduce whether the switching is actually promoted by the high bias voltage itself (*i.e.*, by electrostatic field in the junction) or by high transport current associated with increased bias. The addition energy E_C for form A estimated from the size of the Coulomb diamonds is about 75 meV (the size of the Coulomb diamond along the bias axis is $4E_C$ ^[23]). Even smaller Coulomb diamonds (implying smaller HOMO-LUMO gap) for the form B allow us to identify forms A and B as DHA and VHF respectively.^[24] This identification is further supported by an observed light sensitivity of form A (DHA) to be discussed below.

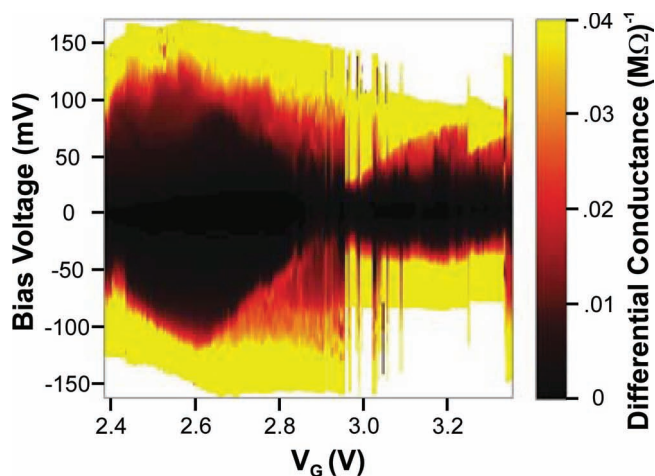


Figure 7. Stability diagram; same data as in Figure 6, but taken for an increased bias range of ± 160 mV.

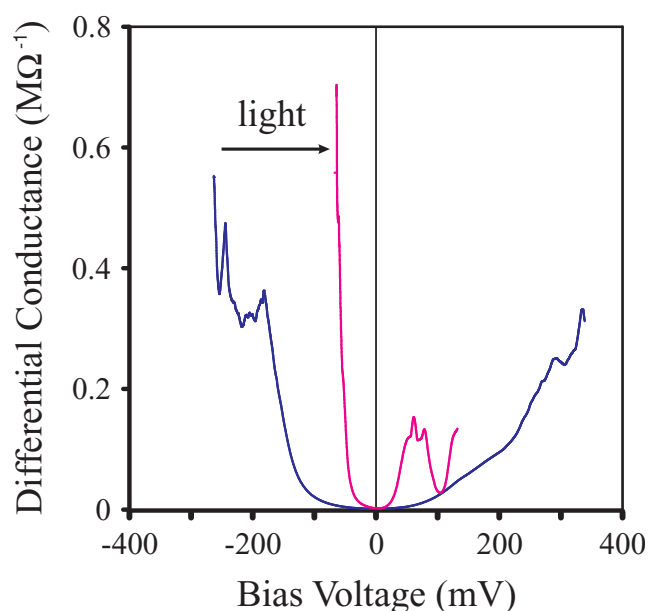


Figure 8. The effect of shining light on molecular junction ($V_G = 2.7$ V). Note the reduced transport gap (zero-current area). Blue curve: DHA; magenta curve: VHF.

At gate voltages not too far from the critical value V_G^0 , the junction was found to be light-sensitive; shining light on the sample for a few minutes (visual light was used) triggered DHA \rightarrow VHF conversion, as shown in Figure 8. Below a gate potential of 2.6 V, the sample was quenched in DHA form and was not light-sensitive. The charge distribution within the molecule in the junction is expected to differ from that of the molecule in solution and photosensitivity will hence reasonably depend on correct tuning of the charge distribution by the gate potential. The future sample evolution after a single light-triggered DHA \rightarrow VHF switching depends on the applied bias voltage: if the bias voltage is kept low (like in Figure 6) the sample stays in VHF (low resistivity) form for indefinitely long time (Figure 9). For higher bias voltages (like in Figure 7), after some time, the sample spontaneously resets back to DHA (high resistivity). It was possible to reset the switch by short-time excursion to high biases, as illustrated in Figure 10. The same light–high bias cycle was repeated many times and more than 20 ON–OFF cycles were recorded, some being presented in Figure 11. It should be noted that all OFF states (DHA form) have similar, though not exactly identical resistance as evident from Figure 11. The same applies to all ON states. It was also possible to reset the switch back to DHA form by increasing the temperature (up to 25 K), as shown in Figure 12.

The above interpretation of junction data as switching between DHA and VHF forms is naturally based on the ready light/heat-induced DHA–VHF conversions occurring in solution. For 1,1-dicyano-2,2-diphenyl-1,2-dihydronaphthalene, a structurally related photochrome comprised of two six-membered rings fused together, it was, however, previously shown that photoinduced C–CN bond dissociation (heterolytic) could occur in polar solvents.^[25] We cannot exclude that such a competing reaction channel could be in play for DHA in the junction at some gate and bias potentials.

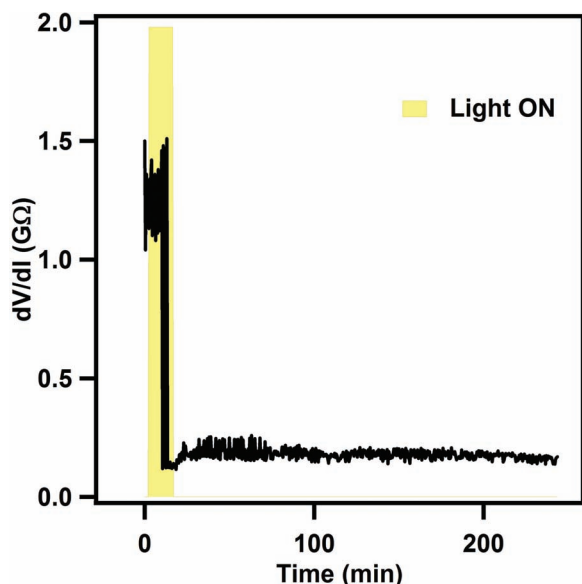


Figure 9. Differential resistance dV/dI versus time ($V_G = 2.67$ V). For each point on the plot a single $I(V)$ curve was taken for bias voltages $V = \pm 100$ mV and the differential resistance for the bias voltage $V = 25$ mV was computed numerically. The highlighted background (yellow) indicates the time interval when the sample (DHA) was illuminated with light. After a single light-triggered switching event the sample stayed in low-resistive state (VHF) for indefinitely long time.

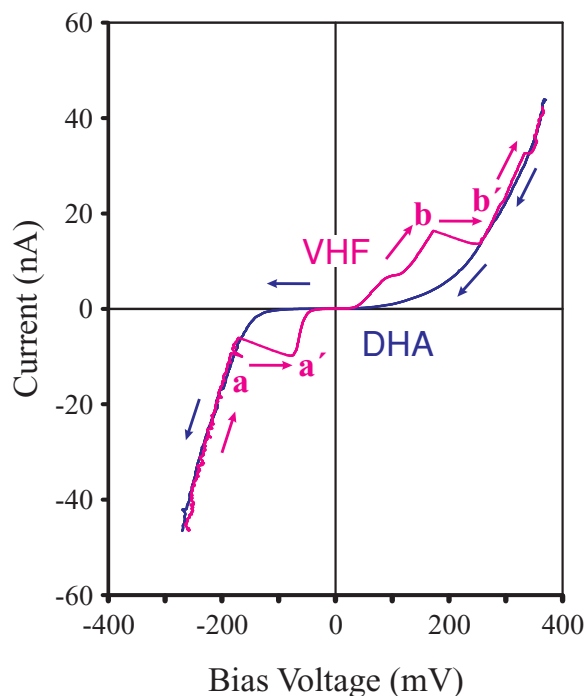


Figure 10. Two $I(V)$ curves taken for a bias scan in negative-to-positive voltage (magenta) and positive-to-negative (blue) directions ($V_G = 2.7$ V). The sample was illuminated all the time. Transition $a \rightarrow a'$ is light-triggered DHA \rightarrow VHF switching event. An excursion to high bias region promoted $b \rightarrow b'$ transition back to DHA form. Many trace-retrace scans were taken. Positions for both $a \rightarrow a'$ and $b \rightarrow b'$ transitions varied from scan to scan, though the reverse one ($b \rightarrow b'$) always happened at bias voltages $|V| > 100$ mV. One representative scan with conveniently placed forward/backward transitions was selected for display.

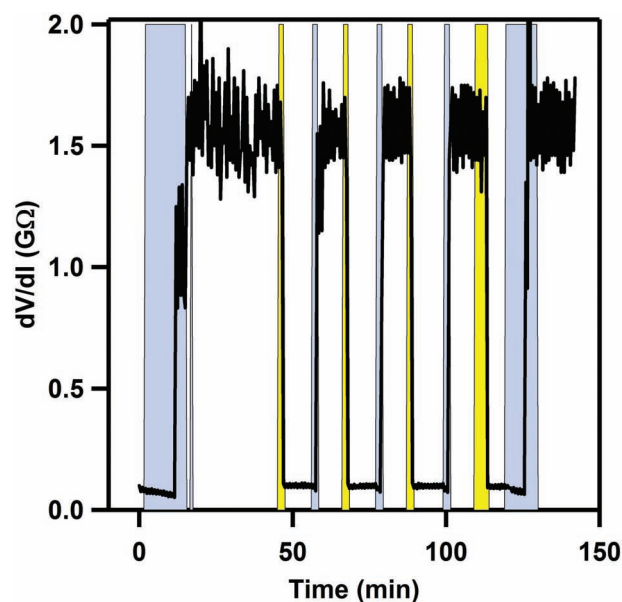


Figure 11. A series of ON-OFF switchings ($V_G = 2.67$ V). The highlighted background indicates the time intervals when the sample was illuminated with light (yellow) or the bias voltage was increased to 80 mV (blue). The differential resistance dV/dI was taken at the bias voltage $V = 25$ mV for both ON (VHF) and OFF (DHA) states.

3. Conclusions

In conclusion, we have developed synthetic protocols for functionalizing the DHA/VHF system with $p\text{-MeSC}_6\text{H}_4$ end-groups, employing Suzuki cross-coupling reactions. Our regioselective

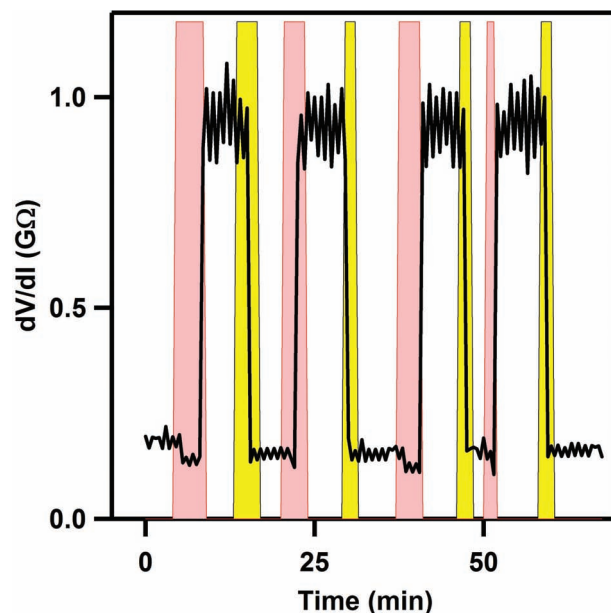


Figure 12. A series of ON-OFF switchings ($V_G = 2.7$ V). The highlighted background indicates the time intervals when the sample was illuminated with light (yellow) or the temperature was increased from 4 K to 25 K (rose). The differential resistance dV/dI was taken at the bias voltage $V = 25$ mV for both ON (VHF) and OFF (DHA) states.

bromination–elimination–cross-coupling protocol for functionalizing the DHA at position 7 was hence successfully expanded to other DHA starting materials via two different routes. While the reactions seemed to work efficiently, purification of the final DHA products turned out significantly more tedious than we have previously experienced with these light-sensitive compounds. From kinetics studies on the thermal ring-closure of VHF to DHA in solution, we have found that the MeS substituent exerts a retarding effect when situated as a *para*-substituent on a phenyl attached to the seven-membered ring for this particular example. A DHA with one MeS anchoring group was successfully placed in the nanogap between silver source and drain electrodes, and the sample was subjected to a variety of conductivity measurements. The molecule was weakly coupled to one electrode, and reversible switching between two forms, most likely DHA (high resistivity, OFF state) and VHF (low resistivity, ON state), was successfully controlled by gate voltage, bias voltage, temperature, and light. In previous work we showed that DHA **2a** was well coupled to at least one electrode as no gate-induced conductance nor Coulomb blockade effects were observed. It seems obvious to grant the MeS substituent in **4a** for the desired weak molecule-electrode coupling, although we can, of course, only speculate on how the molecule is attached to the electrode. The rich switching behavior warrants further exploration of this system in molecular electronics.

4. Experimental Section

General Methods: Reactions under argon atmosphere were performed in a closed vessel equipped with an argon balloon. All reactions using palladium catalyst were performed in a solvent flushed with argon, by flushing argon through the solvent for at least 20 minutes while exposing it to ultrasound. NMR Spectra were acquired on a 300 MHz instrument or a 500 MHz instrument equipped with a cryoprobe. All chemical shift values in ^1H - and ^{13}C NMR spectra are referenced to the solvent (CDCl_3 $\delta_{\text{H}} = 7.26$ ppm, $\delta_{\text{C}} = 77.16$ ppm. CD_3CN $\delta_{\text{H}} = 1.96$ ppm, $\delta_{\text{C}} = 1.94$ ppm. $\text{DMSO}-d_6$ $\delta_{\text{H}} = 2.50$ ppm, $\delta_{\text{C}} = 39.52$ ppm). Thin layer chromatography (TLC) was carried out on commercially available, precoated plates (silica 60) with fluorescence indicator; a color change from yellow to red or violet upon irradiation with UV-light indicated the presence of a DHA. Dry column vacuum chromatography is described in Ref. [26]. All melting points are uncorrected. All spectroscopic measurements (including photolysis) were performed in a 1-cm path length cuvette. Photoswitching experiments were performed using a 150-W xenon arc lamp equipped with a monochromator; the DHA absorption maximum (lowest energy absorption) for each individual species was chosen as the wavelength of irradiation (line width ± 2.5 nm). The thermal back-reaction was performed by heating the sample (cuvette) by a Peltier unit in the UV-vis spectrophotometer. Light-heat cycles described above correspond to the following steps: i) irradiation of the DHA species until no further changes in the absorption spectrum were observed, ii) heating of the formed VHF species until no further changes in the absorption spectrum were observed. A detailed description of the experiment and investigation of the accuracy has previously been published.^[20] A single-molecule junction based on DHA **4a** was prepared according to a previous fabrication method.^[15–17,22]

2-[4'-Methylthio(1,1'-biphenyl)-4-yl]-7-[4-(methylthio)phenyl]-1,8a-dihydroazulene-1,1-dicarbonitrile (3a**):** Compound **10a** (1/4 of a batch made in 2 steps from 1.00 mmol **4a**) was dissolved in toluene (20 mL) flushed with argon. Argon-flushed water (10 mL) was added. The boronic acid (84 mmol, 0.50 mmol), $\text{KF}\cdot 2\text{H}_2\text{O}$ (23.5 mg, 0.25 mmol),

and $\text{Pd}(\text{PPh}_3)_4$ (70 mg, 60 μmol , 25 mol%) were added, and the reaction mixture was stirred at 90 °C overnight. The reaction mixture was diluted with toluene (100 mL), washed with water (2×50 mL) and brine (50 mL), dried with MgSO_4 , filtered, and the solvent was evaporated *in vacuo*. Purification by dry column vacuum chromatography (SiO_2 , 12.6 cm^2 , 0% - 100% CHCl_3 /heptanes, 7% steps, 25 mL fractions) gave **3a** (106.6 mg, 0.213 mmol, 85%, > 90% purity) as a yellow to red solid. Recrystallization from acetonitrile (30–50 mL) afforded **3a** (21.6 mg, 17%) as yellow needles. Crystals suitable for X-ray crystallography were grown from acetonitrile. M.p. 150 °C (decomp.). ^1H NMR (500 MHz, CD_3CN) δ 7.89 (d, $J = 8.7$ Hz, 2H), 7.80 (d, $J = 8.7$ Hz, 2H), 7.67 (d, $J = 8.5$ Hz, 2H), 7.37 (d, $J = 8.5$ Hz, 2H), 7.37 (d, $J = 8.6$ Hz, 2H); 7.28 (d, $J = 8.6$ Hz, 2H), 7.21 (s, 1H), 6.87 (dd, $J = 11.6$, 6.1 Hz, 1H), 6.77 (d, $J = 11.6$ Hz, 1H), 6.48 (dd, $J = 6.1$, 1.6 Hz, 1H), 5.96 (d, $J = 4.5$ Hz, 1H), 3.88 (dd, $J = 4.5$, 1.6 Hz, 1H), 2.53 (s, 3H), 2.49 (s, 3H) ppm. ^{13}C NMR (125 MHz, CD_3CN) δ 143.1, 142.3, 141.6, 140.6, 140.3, 140.0, 138.5, 137.4, 134.2, 133.9, 132.7, 130.9, 129.4, 128.8, 128.7, 128.3, 127.9, 127.6, 122.2, 117.7, 116.8, 114.8, 52.0, 46.6, 15.9 ppm. Elem. anal. calc. for $\text{C}_{32}\text{H}_{24}\text{N}_2\text{S}_2$ (500.68): C 76.76%, H 4.83%, N 5.60%; found: C 76.63%, H 4.48%, N 5.86%. MS (MALDI-): $m/z = 500$ [M^+]. UV-vis (MeCN): λ_{DHA} (ϵ): 376 nm ($21 \times 10^3 \text{ M}^{-1} \text{ cm}^{-1}$). λ_{VHF} (ϵ): 504 nm ($23 \times 10^3 \text{ M}^{-1} \text{ cm}^{-1}$).

2-[4'-Methylthio(1,1'-biphenyl)-4-yl]-1,8a-dihydroazulene-1,1-dicarbonitrile (4a**):** Compound **6a** (1.23 mg, 3.17 mmol) was dissolved in toluene (75 mL) and the solution was flushed with argon for 60 min. Water (50 mL) was added and the mixture was flushed with argon for an additional 30 min. The boronic acid **9** (596 mg, 3.55 mmol), $\text{KF}\cdot 2\text{H}_2\text{O}$ (365 mg, 3.88 mmol), and $\text{Pd}(\text{PPh}_3)_4$ (652 mg, 0.56 mmol) were added, and the reaction mixture was stirred for 48 h at 90 °C. The resulting dark yellow to black reaction mixture was diluted with toluene (200 mL) and allowed to cool to rt. The solution was washed with sat. aqueous NH_4Cl , dried with MgSO_4 , and filtered. Any precipitation on the glassware was dissolved in chloroform, which was then dried with MgSO_4 . The combined organic phases were evaporated on Celite. Purification by dry column vacuum chromatography (SiO_2 , 12.6 cm^2 , 0% - 100% CHCl_3 /heptanes, 5% steps, 25 mL fractions) gave **4a** (960 mg, 80%, >90% purity) as a yellow powder. Recrystallization from acetonitrile gave **4a** (505 mg, 1.34 mmol, 42%) as a bright yellow powder. M.p. 161.8 - 166.5 °C. ^1H NMR (500 MHz, CDCl_3) δ 7.80 (d, $J = 8.6$ Hz, 2H), 7.68 (d, $J = 8.6$ Hz, 2H), 7.56 (d, $J = 8.6$ Hz, 2H), 7.35 (d, $J = 8.6$ Hz, 2H), 6.92 (s, 1H), 6.58 (dd, $J = 11.3$, 6.4 Hz, 1H), 6.48 (dd, $J = 11.3$, 6.1 Hz, 1H), 6.35 (dd, $J = 6.4$, 0.8 Hz, 1H), 6.32 (ddd, $J = 10.2$, 6.1, 2.1 Hz, 1H), 5.84 (dd, $J = 10.2$, 3.8 Hz, 1H), 3.81 (dt, $J = 3.8$, 2.1 Hz, 1H), 2.54 (s, 3H) ppm. ^{13}C NMR (125 MHz, CDCl_3) δ 142.1, 139.9, 138.9, 138.9, 136.5, 132.2, 131.1, 131.0, 129.3, 127.8, 127.6, 127.4, 127.0, 126.9, 121.1, 119.6, 115.3, 112.9, 51.3, 45.3, 15.8 ppm. Elem. anal. calc. for $\text{C}_{25}\text{H}_{18}\text{N}_2\text{S}$ (378.49): C 79.33%, H 4.79%, N 7.40%; found: C 78.71%, H 4.68%, N 7.21%. MS (FAB+): $m/z = 378$ [M^+]. UV-vis (MeCN): λ_{DHA} (ϵ): 376 nm ($28 \times 10^3 \text{ M}^{-1} \text{ cm}^{-1}$). λ_{VHF} (ϵ): 475 nm ($23 \times 10^3 \text{ M}^{-1} \text{ cm}^{-1}$).

2-(4'-Iodophenyl)-7,8-dibromo-7,8,1,8a-tetrahydroazulene-1,1-dicarbonitrile (7**):** Compound **6a** (429.3 mg, 1.123 mmol) was dissolved in CH_2Cl_2 (15 mL) under an argon atmosphere, and the mixture was excluded from light. The reaction mixture was cooled to -78 °C and a solution of Br_2 in CH_2Cl_2 (1.44 mL, 0.78 M, 1.12 mmol) was added dropwise. The brown mixture was then stirred for 1 h after which the solution took a yellow color. Evaporation of the solvents gave **7** (608.7 mg, 1.12 mmol, > 99%) as a yellow to brown foam. ^1H NMR (300 MHz, CDCl_3) δ 7.85–7.79 (m, 2H), 7.50–7.44 (m, 2H), 6.98 (s, 1H), 6.29 (dd, $J = 7.5$, 2.3 Hz, 1H), 6.09 (dd, $J = 12.2$, 7.5 Hz, 1H), 5.93 (dd, $J = 12.2$, 5.5 Hz, 1H), 5.33–5.27 (m, 1H), 5.05–5.01 (m, 1H), 4.65 (br s, 1H) ppm. ^{13}C NMR (75 MHz, CDCl_3) δ 144.3 (two signals), 138.7, 134.7, 129.6, 129.0, 127.8, 125.8, 121.8, 114.5, 111.6, 109.9, 96.8, 53.2, 51.5, 49.1, 44.5 ppm (one signal missing due to overlap). Elem. anal. calc. for $\text{C}_{18}\text{H}_{11}\text{Br}_2\text{IN}_2$ (542.01): C 39.98%, H 2.05%, N 5.17%; found: C 39.68%, H 1.94%, N 5.01%.

7-Bromo-2-(4'-iodophenyl)-1,8a-dihydroazulene-1,1-dicarbonitrile (8a**):** Freshly prepared dibromide **7** (609 mg, 1.12 mmol) was dissolved in dry THF (12 mL, <15 ppm H_2O) under argon atmosphere. The solution

was cooled to 0 °C and a solution of LiHMDS (1.1 mL, 1.1 mmol, 1.0 M) in THF was added dropwise. The reaction mixture was stirred for 2 h, while the temperature was allowed to reach rt. The reaction mixture was diluted with Et₂O (100 mL), washed with aqueous NH₄Cl (2 × 50 mL), dried with MgSO₄, and filtered. Evaporation of the solvents gave **8a** (516 mg, >90% purity) as a black solid with minor impurities. An analytically pure sample was obtained by purification by dry column chromatography (SiO₂, 12.6 cm², 0–30% THF/ heptanes, 5% steps, 40 mL fractions) followed by recrystallization from CH₂Cl₂/ heptanes, which gave **8a** as discolored yellow needles. M.p. 168 °C (decomp.). ¹H NMR (500 MHz, CDCl₃) δ 7.83 (d, *J* = 8.7 Hz, 2H), 7.45 (d, *J* = 8.7 Hz, 2H), 6.90 (s, 1H), 6.58–6.49 (m, 2H), 6.34 (d, *J* = 5.9 Hz, 1H), 6.11 (d, *J* = 4.4 Hz, 1H), 3.79 (dd, *J* = 4.4, 1.8 Hz, 1H) ppm. ¹³C NMR (125 MHz, CDCl₃) δ 140.8, 140.7, 138.7, 133.3, 132.3, 132.1, 129.6, 127.9, 120.7, 120.3, 120.1, 114.5, 112.3, 97.1, 51.1, 44.6 ppm. Elem. anal. calc. for C₁₈H₁₀BrIn₂ (461.09): C 46.89%, H 2.19%, N 6.08%; found: C 46.63%, H 2.05%, N 6.03%. MS (EI⁺): *m/z* = 460 [M⁺]. UV-vis (MeCN): λ_{DHA} (ε): 363 nm (21 × 10³ M⁻¹ cm⁻¹). λ_{VHF} (ε): 468 nm (27 × 10³ M⁻¹ cm⁻¹).

2-[4'-Methylthio(1,1'-biphenyl)-4-yl]-7-bromo-1,8a-dihydroazulene-1,1-dicarbonitrile (**10a**): Freshly prepared dibromide **11** (from 1.00 mmol **4a**) was dissolved dry THF (20 mL) and cooled to 0 °C. A solution of LiHMDS in THF (1.00 mL, 1.00 mmol, 1.0 M) was added dropwise. After addition of 0.1 mL the solution changed color from dark green to yellow. Addition of the rest of the base caused a color change to black. The reaction mixture was stirred for 1 h, while the temperature was allowed to reach rt. The reaction mixture was then diluted with Et₂O (100 mL), washed with brine (100 mL), dried with MgSO₄, and filtered. Evaporation of the solvents gave **10a** (>90% purity) as a black solid. An analytically pure sample was obtained by dry column vacuum chromatography (SiO₂, 12.6 cm², 0% - 22% THF/ heptanes, 1% steps, 40 mL fractions), which gave **10a** (74% recovered, > 95% purity) as a yellow solid. A subsequent recrystallization from acetonitrile gave **10a** (12% recovered) as yellow crystals. M.p. 154 °C (decomp.). ¹H NMR (500 MHz, CDCl₃) δ 7.80 (d, *J* = 8.7 Hz, 2H), 7.69 (d, *J* = 8.7 Hz, 2H), 7.56 (d, *J* = 8.6 Hz, 2H), 7.35 (d, *J* = 8.6 Hz, 2H), 6.92 (s, 1H), 6.54 (m, 2H), 6.33 (dt, *J* = 4.1, 1.8 Hz, 1H), 6.14 (d, *J* = 4.4 Hz, 1H), 3.82 (dd, *J* = 4.4, 1.8 Hz, 1H), 2.54 (s, 3H) ppm. ¹³C NMR (125 MHz, CDCl₃) δ 142.7, 141.4, 141.2, 139.2, 136.3, 132.9, 132.2, 131.3, 128.8, 127.6, 127.5, 127.1, 127.0, 120.3, 120.0, 120.0, 114.8, 112.5, 51.2, 44.7, 15.8 ppm. Elem. anal. calc. for C₂₅H₁₇BrN₂S (457.38): C 65.65%, H 3.75%, N 6.12%; found: C 65.24%, H 3.65%, N 6.40%. MS (EI⁺): *m/z* = 456/ 458 [M⁺, ^{79/81}Br]. UV-vis (MeCN): λ_{DHA} (ε): 380 nm (45 × 10³ M⁻¹ cm⁻¹). λ_{VHF} (ε): 462 nm (37 × 10³ M⁻¹ cm⁻¹).

2-[4'-Methylthio(1,1'-biphenyl)-4-yl]-7,8-dibromo-1,7,8,8a-tetrahydroazulene-1,1-dicarbonitrile (**11**): Compound **4a** (378.5 mg, 1.00 mmol) was dissolved in CH₂Cl₂ (20 mL). The solution was cooled to -78 °C and stirred for 20 min. A solution of Br₂ in CH₂Cl₂ (1.28 mL, 1.00 mmol, 0.78 M) was added dropwise, and the reaction mixture was stirred for 1 h. The dry ice/ acetone bath was removed and the temperature was allowed to rise to rt. Evaporation of the solvent gave **11** (538.3 mg, 1.00 mmol, >99%) as a green solid/ foam. M.p. 135 °C (decomp.). ¹H NMR (500 MHz, CDCl₃) δ 7.82 (d, *J* = 8.6 Hz, 2H), 7.69 (d, *J* = 8.6 Hz, 2H), 7.56 (d, *J* = 8.4 Hz, 2H), 7.35 (br d, *J* = 8.4 Hz, 2H), 7.01 (s, 1H), 6.28 (dd, *J* = 7.6, 2.2 Hz, 1H), 6.10 (dd, *J* = 12.2, 7.6 Hz, 1H), 5.92 (dd, *J* = 12.2, 5.5 Hz, 1H), 5.35–5.31 (m, 1H), 5.07 (dt, *J* = 3.0, 1.5 Hz, 1H), 4.68 (br s, 1H), 2.54 (s, 3H) ppm. Elem. anal. calc. for C₂₅H₁₈Br₂N₂S (538.30): C 55.78%, H 3.37%, N 5.20%; found: C 55.54%, H 3.24%, N 5.16%.

Crystallographic data (excluding structure factors) for the structure(s) reported in this paper have been deposited with the Cambridge Crystallographic Data Centre as supplementary publication no. CCDC-857551 (**10a**), CCDC-857550 (**3a**), CCDC-857552 (**13a**).

Supporting Information

Supporting Information is available from the Wiley Online Library or from the author.

Acknowledgements

The research leading to these results has received funding from the European Community's Seventh Framework Programme (FP7/2007-2013) under the grant agreement "SINGLE" no 213609, coordinated by Prof. T. Bjørnholm who is thanked for helpful discussions. In addition, support from The Danish Council for Independent Research | Natural Sciences (#10-082088) and the Swedish Research Council is acknowledged.

Received: March 29, 2012

Revised: May 17, 2012

Published online: June 19, 2012

- [1] a) L. Carroll, C. B. Gorman, *Angew. Chem. Int. Ed.* **2002**, *41*, 4378; b) N. Robertson, C. A. McGowan, *Chem. Soc. Rev.* **2003**, *32*, 96; c) A. C. Benniston, *Chem. Soc. Rev.* **2004**, *33*, 573; d) A. Troisi, M. A. Ratner, *Small* **2006**, *2*, 172; e) N. Weibel, S. Grunder, M. Mayor, *Org. Biomol. Chem.* **2007**, *5*, 2343; f) R. Klajn, J. F. Stoddart, B. A. Grzybowski, *Chem. Soc. Rev.* **2010**, *39*, 2203; g) S. J. van der Molen, P. Liljeroth, *J. Phys.: Condens. Matter* **2010**, *22*, 133001.
- [2] A. V. Danilov, P. Hedegård, D. S. Golubev, T. Bjørnholm, S. E. Kubatkin, *Nano Lett.* **2008**, *8*, 2393.
- [3] a) D. Dulic, S. J. van der Molen, T. Kudernac, H. T. Jonkman, J. J. D. de Jong, T. N. Bowden, J. van Esch, B. L. Feringa, B. J. van Wees, *Phys. Rev. Lett.* **2003**, *91*, 207402; b) N. Katsonis, T. Kudernac, M. Walko, S. J. van der Molen, B. J. van Wees, B. L. Feringa, *Adv. Mater.* **2006**, *18*, 1397; c) C. Zhang, Y. He, H.-P. Cheng, Y. Xue, M. A. Ratner, X.-G. Zhang, P. Krstic, *Phys. Rev. B* **2006**, *73*, 125445; d) A. C. Whalley, M. L. Steigerwald, X. Guo, C. Nuckolls, *J. Am. Chem. Soc.* **2007**, *129*, 12590; e) A. S. Kumar, T. Ye, T. Takami, B.-C. Yu, A. K. Flatt, J. M. Tour, P. S. Weiss, *Nano Lett.* **2008**, *8*, 1644; f) V. Ferri, M. Elbing, G. Pace, M. D. Dickey, M. Zharnikov, P. Samorì, M. Mayor, M. A. Rampi, *Angew. Chem. Int. Ed.* **2008**, *47*, 3407; g) A. J. Kronemeijer, H. B. Akkerman, T. Kudernac, B. J. van Wees, B. L. Feringa, P. W. M. Blom, B. de Boer, *Adv. Mater.* **2008**, *20*, 1467; h) S. J. van der Molen, J. Liao, T. Kudernac, J. S. Augustsson, L. Bernard, M. Calame, B. J. van Wees, B. L. Feringa, C. Schönenberger, *Nano Lett.* **2009**, *9*, 76; i) W. R. Browne, B. Feringa, *Annu. Rev. Phys. Chem.* **2009**, *60*, 407; j) T. Kudernac, N. Katsonis, W. R. Browne, B. L. Feringa, *J. Mater. Chem.* **2009**, *19*, 7168; k) T. Tsujioka, M. Irie, *J. Photochem. & Photobiol. C: Photochem. Rev.* **2010**, *11*, 1.
- [4] a) M. Zhuang, M. Ernzerhof, *Phys. Rev. B* **2005**, *72*, 073104; b) M. Zhuang, M. Ernzerhof, *J. Chem. Phys.* **2009**, *130*, 114704.
- [5] S. Lara-Avila, A. V. Danilov, S. E. Kubatkin, S. L. Broman, C. R. Parker, M. B. Nielsen, *J. Phys. Chem. C* **2011**, *115*, 18372.
- [6] J. Daub, T. Knöchel, A. Mannschreck, *Angew. Chem. Int. Ed. Engl.* **1984**, *23*, 960.
- [7] a) S. L. Broman, M. Å. Petersen, C. G. Tortzen, A. Kadziola, K. Kilså, M. B. Nielsen, *J. Am. Chem. Soc.* **2010**, *132*, 9165; b) M. Å. Petersen, S. L. Broman, K. Kilså, A. Kadziola, M. B. Nielsen, *Eur. J. Org. Chem.* **2011**, 1033.
- [8] H. Görner, C. Fischer, S. Gierisch, J. Daub, *J. Phys. Chem.* **1993**, *97*, 4110.
- [9] a) J. Daub, S. Gierisch, J. Salbeck, *Tetrahedron Lett.* **1990**, *31*, 3113; b) J. Achatz, C. Fischer, J. Salbeck, J. Daub, *J. Chem. Soc., Chem. Commun.* **1991**, 504; c) M. Å. Petersen, L. Zhu, S. H. Jensen, A. S. Andersson, A. Kadziola, K. Kilså, M. B. Nielsen, *Adv. Funct. Mater.* **2007**, *17*, 797.
- [10] C. R. Parker, C. G. Tortzen, S. L. Broman, M. Schau-Magnussen, K. Kilså, M. B. Nielsen, *Chem. Commun.* **2011**, *47*, 6102.

- [11] V. De Waele, M. Beutter, U. Schmidhammer, E. Riedle, J. Daub, *Chem. Phys. Lett.* **2004**, 390, 328.
- [12] a) H. van Houten, C. W. J. Beenakker, A. A. M. Staring, in *Single Charge Tunnelling and Coulomb Blockade Phenomena in Nanostructures*, Plenum, New York **1992**, Ch. 5; b) H. Park, J. Park, A. K. L. Lim, E. H. Anderson, A. P. Alivisatos, P. McEuen, *Nature* **2000**, 407, 57.
- [13] K. Nørgaard, M. B. Nielsen, T. Bjørnholm, in *Functional Organic Materials* (Eds: T. J. J. Müller, U. H. F. Bunz), VCH-Wiley, Weinheim **2007**, p. 353–392.
- [14] a) Y. J. Kwon, S. B. Lee, K. Kim, M. S. Kim, *J. Mol. Struct.* **1994**, 318, 25; b) J. Hu, D. L. Mattern, *J. Org. Chem.* **2000**, 65, 2277; c) L. Zobbi, M. Mannini, M. Pacchioni, G. Chastanet, D. Bonacchi, C. Zanardi, R. Biagi, U. Del Pennino, D. Gatteschi, A. Cornia, R. Sessoli, *Chem. Commun.* **2005**, 1640; d) Y. S. Park, A. C. Whalley, M. Kamenetska, M. L. Steigerwald, M. S. Hybertsen, C. Nuckolls, L. Venkataraman, *J. Am. Chem. Soc.* **2007**, 129, 15768.
- [15] a) S. Kubatkin, A. Danilov, M. Hjort, J. Cornil, J.-L. Brédas, N. Stühr-Hansen, P. Hedegård, T. Bjørnholm, *Nature* **2003**, 425, 698; b) S. Kubatkin, A. Danilov, M. Hjort, J. Cornil, J.-L. Brédas, N. Stühr-Hansen, P. Hedegård, T. Bjørnholm, *Current Appl. Phys.* **2004**, 4, 554.
- [16] A. V. Danilov, S. E. Kubatkin, S. G. Kafanov, T. Bjørnholm, *Faraday Discuss.* **2006**, 131, 337.
- [17] S. Lara-Avila, A. Danilov, V. Geskin, S. Bouzakraoui, S. Kubatkin, J. Cornil, T. Bjørnholm, *J. Phys. Chem. C* **2010**, 114, 20686.
- [18] L. Gobbi, P. Seiler, F. Diederich, V. Gramlich, C. Boudon, J.-P. Gisselbrecht, M. Gross, *Helv. Chim. Acta* **2001**, 84, 743.
- [19] M. Å. Petersen, S. L. Broman, A. Kadziola, K. Kilså, M. B. Nielsen, *Eur. J. Org. Chem.* **2009**, 2733.
- [20] S. L. Broman, S. L. Brand, C. R. Parker, M. Å. Petersen, C. G. Tortzen, A. Kadziola, K. Kilså, M. B. Nielsen, *Arkivoc* **2011**, ix, 51.
- [21] D. H. McDaniel, H. C. Brown, *J. Org. Chem.* **1958**, 23, 420.
- [22] a) S. E. Kubatkin, A. V. Danilov, H. Olin, T. Claeson, *Appl. Phys. Lett.* **1998**, 73, 3604; b) S. E. Kubatkin, A. V. Danilov, H. Olin, T. Claeson, *J. Low Temp. Phys.* **2000**, 118, 307; c) A. V. Danilov, D. S. Golubev, S. E. Kubatkin, *Phys. Rev. B* **2002**, 65, 1253121.
- [23] L. P. Kouwenhoven, D. G. Austing, S. Tarucha, *Rep. Prog. Phys.* **2001**, 64, 701.
- [24] The junction properties (conductance and the phase of Coulomb blockade oscillations) for form B were not as stable as for form A. Therefore we could not extract from our data the exact value for the addition energy for form B, but qualitatively, it is quite clear from Figure 7 that the addition energy is reduced after A → B switching.
- [25] H. Görner, T. Mrozek, J. Daub, *Chem. Eur. J.* **2002**, 8, 4008.
- [26] D. S. Pedersen, C. Rosenbohm, *Synthesis* **2001**, 2431.